Evolution of Pt-Ru Catalysts from Molecular Precursors to Bimetallic Nanoparticles

A.I.Frenkel, M.S.Nashner, C.W.Hills, R.G.Nuzzo and J.R.Shapley

University of Illinois at Urbana-Champaign

One of the major problems in developing a predictive understanding of the structure and reactivity of supported bimetallic catalysts is the limited control of the particle size and/or compositional distributions obtained during their synthesis by the most commonly used co-impregnation methods. An attractive alternative to these methods is the use of molecular cluster compounds as precursors, which, upon their conversion, predetermines the proper stoichiometry of the metal atoms in the cluster. Representative carbon-supported [PtRu$_5$]/C nanoparticles, which are of interest for anode catalysts for methanol electro-oxidation, were synthesized from molecular cluster precursors PtRu$_5$C(CO)$_{16}$ at the University of Illinois at Urbana-Champaign. The average composition of the particles was determined by energy dispersive X-ray analysis (EDX) and found to be indistinguishable from the stoichiometry of the precursor. The distribution of Ru composition over 140 particles from different sample regions was exceptionally narrow, with a FWHM of 3%. The particle size (16 Å) and its distribution (FWHM of 5 Å) were measured by STEM. The "long-range" structure of the nanoparticles was obtained to be *fcc* by electron microdiffraction. The desorption of the CO ligands and formation of an increasingly metallic state were followed by temperature-programmed reaction spectroscopy (TPRS) measurements.

Our *in-situ* XAFS study of the nucleation and growth of these supported Pt-Ru catalysts was aimed to develop an understanding of the most fundamental factors which control the catalytic activity of these nanoclusters. These questions cannot be clarified without the knowledge of the local atomic structure of the clusters, namely: (1) *Is the atomic distribution within the particles random?* The two metals may be fully miscible in the nanoparticle, with or without chemical ordering, or segregate to the surface or to the interior of the cluster (Figure 1). These different scenarios strongly affect the catalytic activity of the particles. (2) *What are the stages of progressive reconstruction of the particles during the condensation from the precursor?* During the nucleation and growth, while the metallic character increases and the particle size increases, the bonds between the CO ligands and metals should gradually break. These kinetics likely control the rate and evolution of the original precursor structure to the
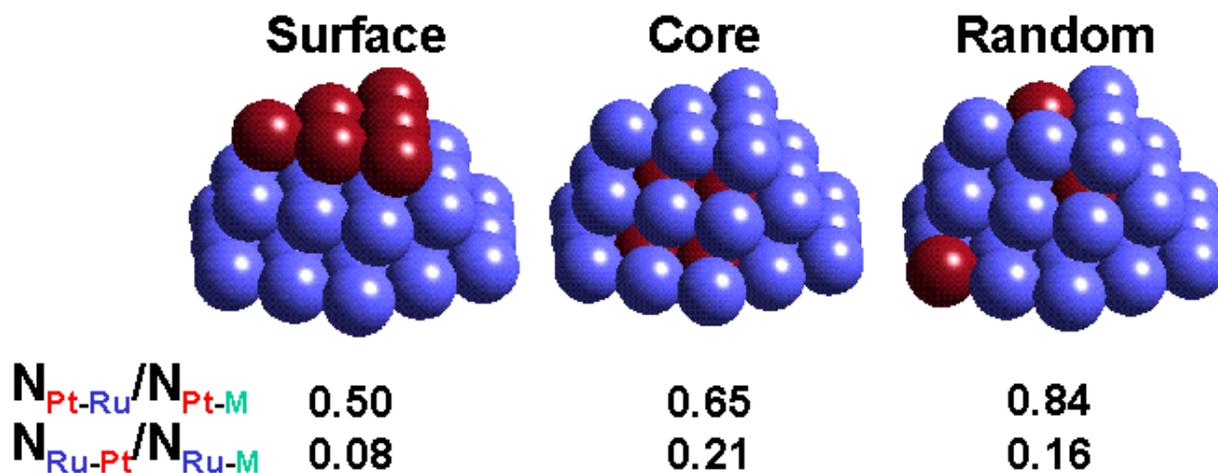
Figure 1. Three scenarios of atomic distribution in a 37-atom, heterometallic (5:1) nanoparticle. The *fcc* hemispherical cuboctahedron structure, with an edge length of 3 atoms, illustrates the difference in the relative Pt-Ru and Ru-Pt coordination numbers, normalized by the total Pt-M and Ru-M coordination numbers, respectively. The primary model fitting criterion is agreement with experimentally determined coordination numbers. For example, for the fully reduced [PtRu$_5$] cluster, the obtained relative coordination numbers (0.4 ± 0.3 for Pt and 0.12 ± 0.03 for Ru) indicate surface segregation of Pt atoms.

final metal particle. (3) What are the effects of the support? The role played by the support is to mediate the transport-limited aggregation of the precursor clusters, which condense to form the final metal nanoparticles. The study of different support materials should help to design the catalysts with the pre-defined level of alloying and thus the qualities of the final metallic state.

We performed the XAFS experiment at the NSLS X16C beamline. The sample preparation and the experimental setup are described in the literature[1,2]. We used a custom designed and built catalyst cell, which allowed simultaneous *in-situ* X-ray fluorescence and transmission measurements over an operating temperature range 150 – 773 K. The carbon-supported PtRu$_5$C(CO)$_{16}$ precursor samples were activated by heating at a rate of 15 K/min in flowing H$_2$ to several temperatures: 423 K, 473 K,

Figure 2. Fourier transform magnitudes of the k^3-weighted, Pt L$_3$-edge and Ru K-edge EXAFS data measured at 190 K from the carbon-supported [PtRu$_5$] nanoparticles after activation under H$_2$ at different temperatures. Dashed lines indicate the first-shell FEFF6 fit to the metal-metal (M-M) contribution. The ranges corresponding to the contributions of M-O, M-M and collinear M-M-M configurations of atoms are shown for clarity.

573 K and 673 K. They were then cooled rapidly (using liquid nitrogen) to 190 K before making XAFS measurements.

After subtracting the background from the experimental data, the resultant k^3-weighted $\chi(k)$ function was Fourier transformed to R-space (Figure 2). Several conclusions are obvious from visually examining the raw data. First, the notable decrease of the signal amplitude in the R-range below 1.5 Å with the increase of the activation temperature manifests the reduction in the coordination of the metals by the low-Z neighbors, i.e., carbon and oxygen (denoted schematically as Pt-O and Ru-O). This result is consistent with the TPRS measurements, which demonstrate that CO is lost from the cluster across a temperature range between 400-600 K[2]. Second, the increase in the intensity of Pt-M and Ru-M interactions (between 2 and 3 Å) manifests the increase in the cluster size. This result is supported by the STEM measurements, which demonstrate that heating leads to the growth of larger and increasingly more coherent particles across the temperature range[2]. A similar conclusion can be derived from inspecting the R-range between 4 and 5 Å. In the *fcc* structure,

this range is primarily attributed to collinear multiple-scattering (double- and triple-scattering) paths connecting the central atom, its nearest-neighbor, and the next nearest-neighbor in the same direction[3]. The total number of these paths increases with the cluster size, as does the number of the nearest-neighbor M-M interactions. We would like to comment that, although the Debye-Waller factors do alter the amplitude of EXAFS signals measured at different temperatures, the effect discussed above can clearly be attributed solely to the coordination number (and thus cluster size) change (the data were taken at the same temperature, 190 K).

Finally, the Pt L$_3$ – XANES data, measured *in situ* for different support materials[2,4] demonstrated the marked sensitivity of the edge position to the activation temperature. The binding energy shift to lower energies during reduction, i.e., the increase of metallic character of the nanoparticles, is in agreement with the TPRS and STEM data. We found that the electronic structure of the nanoclusters supported on a fullerene soot is dramatically different from the microporous carbon-supported particles[4]. In the former case, the final state of the nanoparticles never reaches

Science Highlights - Chemical Sciences

a limiting "metallic state", i.e., the clusters are not completely reduced. One of the most plausible explanations of this effect is the formation of a Ru-carbide phase[4] at the fullerene-soot support and nanoparticle boundary.

The details of the multiple-scattering, multiple data set refinement of the experimental EXAFS data are described in our earlier reports[1-4]. EXAFS theory for the first nearest-neighbor contributions, calculated with FEFF6[5], was fit in R-space to both the Pt L_3- and Ru K-edge data, simultaneously, using the UWXAFS package[6]. The fits and the numerical results for the first nearest-neighbor coordination numbers and bond lengths are shown in Figures 2 and 3, respectively[2]. The full multiple-scattering analysis was performed for the completely reduced clusters[1], where it was confirmed (by comparing the coordination numbers for the first four Pt-M nearest-neighbor pairs with several structural models) that the final size of the nanoparticles after reduction was ca. 12 Å and the shape of the particle was hemispherical. For comparison, for a model of spherical (i.e., cuboctahedral) particles, the average first nearest-neighbor coordination number of 6.3 would correspond to much smaller particle diameter (<10 Å) than the value measured by STEM. The structure was best fit with the *fcc* model, the same as obtained by electron microdiffraction, which is an intriguing result given that bulk alloys of this composition adopt an *hcp* structure.

The combination of our EXAFS results (Figure 3) with those of XANES, TPRS, STEM, EDX and microdiffraction measurements suggests the following scenario of structural reconstructions during H_2 reduction. Heating the carbon-supported precursor molecules (Figure 4, A) in H_2 resulted in the loss of the CO ligand shell (as established by TPRS, EXAFS and XANES) with substitution of metal-metal bonds and the concomitant increase in cluster size to the maximum of 12 – 16 Å (EXAFS, STEM) with the formation of increasingly metallic state (XANES, STEM, TPRS). The increase in the cluster size with the activation temperature is evident from the increase seen in the coordination number of Ru (majority element) – metal bonds (Figure 3). The increase in the Ru-M coordination and, therefore, the increasing alloying of separate cluster precursors, was also reflected in the changes seen in the average bond distances separating the metals (Figure 3), which all converge toward the value found in the final particle structure. After being heated to 473 K, EXAFS reveals that the Pt atoms have significantly larger first-shell metal coordination numbers than does Ru (Figure 3). This suggests that, during this treatment, the Ru binds to Pt centers (Figure 4 B), which have coalesced to form a core structure at the center of the nanoparticle (see also Figure 1). As the temperature increases further, a significant restructuring of the particles occurs upon annealing in H_2. This final nanoparticle structure (Figure 4 C) has *fcc* symmetry
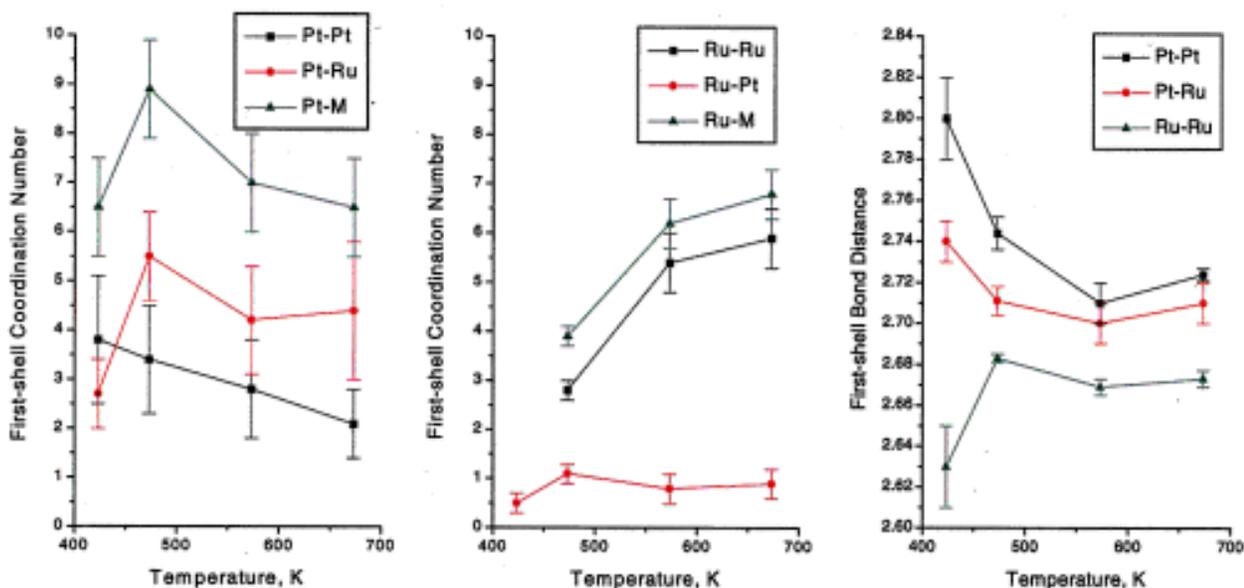
Figure 3. Evolution of the first-shell coordination environment (coordination numbers and bond distances) of Pt-Ru nanoparticles during reduction in H_2.
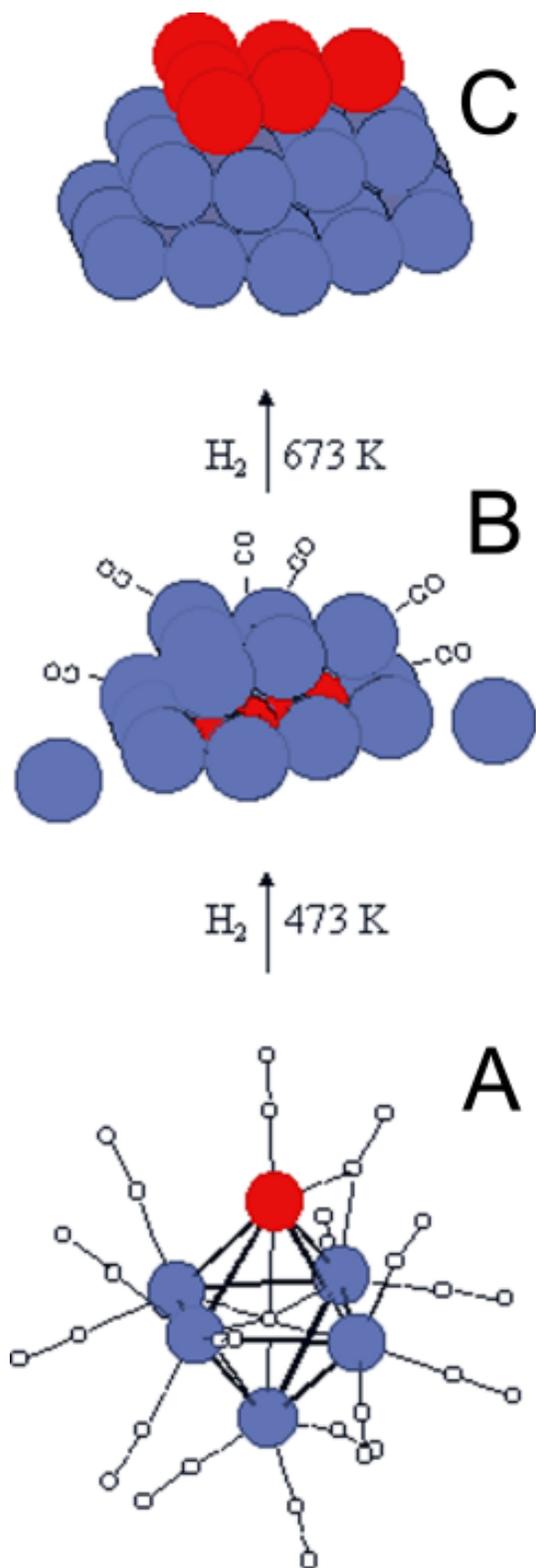
(microdiffraction, EXAFS), hemispherical shape (EXAFS) and exhibits a preferential segregation of Pt towards the surface of the nanoparticles (see also Figure 1). The fact that the EXAFS result for the final particle size (12 Å) is smaller than that obtained by STEM may have an origin in the enhanced disorder of the surface atoms. EXAFS underestimates the particle size (relative to that directly observed from STEM measurements) if the atomic positions of the Pt and Ru particles near the surface or at the interface with the support deviate strongly from the periodic *fcc* structure assumed in the simulations[7].

We believe that the formation of a cherry-like structure with Pt in the core results from the kinetically controlled reductive nucleation of fragmented Ru species onto incipient Pt-rich nanoparticles. One might conclude that this provides a template for the nucleation of the final *fcc* nanoparticles, as opposed to the *hcp* ones predicted by the bulk phase diagram. The facile dynamics of core-shell inversion, however, strongly suggest that the latter limiting structure must, in fact, be thermodynamically directed. This reconstruction of the Pt core, one in which its atoms ultimately segregate to the nanoparticle surface, is likely promoted by differences in the relevant metal-metal bond energies as well as those between Pt and Ru to CO and/or hydrogen. Such energy balances are a very common origin of the structural rearrangements seen in molecular clusters and bimetallic colloids.

References
[1] M.S. Nashner, A.I. Frenkel, D.L. Adler, J.R. Shapley, and R.G. Nuzzo, *J. Am. Chem. Soc.*, **119**, 7760 (1997).
[2] M.S. Nashner, A.I. Frenkel, D. Somerville, C. W. Hills, J.R. Shapley, and R.G. Nuzzo, *J. Am. Chem. Soc.*, **120**, 8093 (1998).
[3] A.I. Frenkel, *J. Synchrotron Rad.*, **6** , 293 (1999).
[4] C.W. Hills, M.S. Nashner, A.I. Frenkel, J.R. Shapley, and R.G. Nuzzo, *Langmuir*, **15**, 690 (1999).
[5] S.I. Zabinsky, J.J. Rehr, A. Ankudinov, R.C. Albers, and M.J. Eller, *Phys. Rev. B*, **52**, 2995 (1995).
[6] E.A. Stern, M. Newville, B. Ravel, Y. Yacoby, and D. Haskel, *Physica B*, **208 & 209**, 117 (1995).
[7] T. Shido and R. Prins, *J. Phys. Chem.*, **102**, 8426 (1998).

Figure 4. Qualitative model of the nucleation and growth processes of carbon-supported [PtRu$_5$] nanoparticles.